PHYSICAL REVIEW C **84**, 047302 (2011)

High-spin yrast states in the γ-soft nuclei ^{135}Pr and ^{134}Ce

E. S. Paul,[1] C. Fox,[1] A. J. Boston,[1] H. J. Chantler,[1] C. J. Chiara,[2,*] R. M. Clark,[3] M. Cromaz,[3] M. Descovich,[1] P. Fallon,[3] D. B. Fossan,[2] A. A. Hecht,[4,†] T. Koike,[2,‡] I. Y. Lee,[3] A. O. Macchiavelli,[3] P. J. Nolan,[3] K. Starosta,[2,§] R. Wadsworth,[5] and I. Ragnarsson[6]

[1]*Oliver Lodge Laboratory, University of Liverpool, Liverpool L69 7ZE, United Kingdom*

[2]*Department of Physics and Astronomy, State University of New York at Stony Brook, Stony Brook, New York 11794, USA*

[3]*Nuclear Science Division, Lawrence Berkeley National Laboratory, Berkeley, California 94720, USA*

[4]*Wright Nuclear Structure Laboratory, Physics Department, Yale University, New Haven, Connecticut 06520, USA*

[5]*Department of Physics, University of York, Heslington, York YO10 5DD, United Kingdom*

[6]*Division of Mathematical Physics, LTH, Lund University, P.O. Box 118, S-22100 Lund, Sweden*

(Received 15 June 2011; published 17 October 2011)

High-spin states have been studied in $^{135}_{59}$Pr, populated through the ^{116}Cd(^{23}Na,4n) reaction at 115 MeV, using the Gammasphere γ-ray spectrometer. The negative-parity yrast band has been significantly extended to spin $\sim 45\hbar$ and excitation energy 21.5 MeV, showing evidence for several rotational alignments. The positive-parity yrast band of $^{134}_{58}$Ce, populated through the $p4n$ channel of this reaction, was also populated to spin $\sim 38\hbar$ and excitation energy 18 MeV. Cranking calculations indicate that these nuclei are soft with respect to the triaxiality parameter γ and that several competing nuclear shapes occur at high spin.

DOI: 10.1103/PhysRevC.84.047302 PACS number(s): 27.60.+j, 23.20.Lv, 21.10.Re

Nonaxial nuclear shapes, described by the triaxiality parameter γ in the polar representation of rotating quadrupole shapes [1], are thought to become important for the $_{57}$La, $_{58}$Ce, $_{59}$Pr, and $_{60}$Nd isotopes beyond $A = 130$ that approach the $N = 82$ shell closure [2–4]. This nonaxial nuclear deformation is induced through core polarization by valence particles in anisotropic orbitals [5,6]. High-j particles from the bottom of a subshell prefer prolate nuclear shapes, while particles from the top of a subshell prefer an oblate shape [7]. The delicate interplay of such valence particles can therefore influence the overall shape of the nucleus, inducing triaxiality. Such is the case for these nuclei where valence protons occupy low-Ω orbitals from the bottom of the $\pi h_{11/2}$ subshell, while valence neutrons occupy high-Ω orbitals from the top of the $\nu h_{11/2}$ subshell. Hence, this mass region provides an ideal environment for studying the shape-driving effects of specific valence particles. In addition, neutrons intruding from above the $N = 82$ shell gap can induce larger quadrupole deformation, ε_2.

The ideal triaxial shape is realized for $\gamma = \pm 30^\circ$ or -90°. In the Lund convention [1], such shapes are equivalent with distinct "long," "short," and "intermediate" principal axes; it is only the axis about which the nucleus rotates that is different. For $\gamma = 30^\circ$, the nucleus rotates about the short axis; for $\gamma = -30^\circ$, the nucleus rotates about the intermediate axis; and for $\gamma = -90^\circ$, it rotates about the long axis. The largest moment of inertia is achieved for $\gamma = 30^\circ$ and hence, classically, a triaxial body minimizes its energy for such motion. For the nucleus, however, which is a finite quantum system, strong coupling between collective and single-particle angular momenta can influence the way in which a triaxial nucleus rotates, or indeed precesses (wobbles) [8].

This Brief Report presents new high-spin results for odd-Z ^{135}Pr, where the yrast band has been significantly extended to $45\hbar$; previous work on this nucleus can be found in Refs. [9–11]. In addition, the yrast band of ^{134}Ce [12,13] has also been extended to spin approaching $40\hbar$.

Experimental Details. High-spin states in ^{135}Pr were populated with the ^{116}Cd(^{23}Na,4$n\gamma$) fusion-evaporation reaction. The experiment was performed at the Lawrence Berkeley National Laboratory, using a 115-MeV ^{23}Na beam supplied by the 88-inch cyclotron. This beam energy was chosen to primarily study the ^{134}Pr nucleus (5n) [14]. Two experiments were performed with different types of targets. A single, thin, self-supporting cadmium target of nominal thickness 1.2 mg/cm^2 was used to study high-spin states, while a 1.0-mg/cm^2 cadmium target on a thick lead backing of 15 mg/cm^2 was used to allow lifetime measurements through the Doppler-shift attenuation method (DSAM) [15]. The Gammasphere γ-ray spectrometer [16,17], containing 99 HPGe detectors, was used to record Compton-suppressed γ-ray coincidence events. Approximately 6×10^8 such events, of average γ-ray fold 4.5, were collected with the thin target, while 1.5×10^9 were collected with the backed target.

In order to provide channel selection, the bismuth germanate (BGO) anti-Compton shield elements of Gammasphere were used as a γ-ray fold and sum-energy selection device [18]. By removing the Hevimet collimators from the front of the HPGe detectors, the front of the BGO suppression shields were exposed, allowing γ rays to strike the shield elements directly. The number of BGO elements firing and

*Present address: Department of Chemistry and Biochemistry, University of Maryland, College Park, Maryland 20742, USA.

†Present address: Department of Chemical and Nuclear Engineering, University of New Mexico, Albuquerque, New Mexico 87131-0001, USA.

‡Present address: Graduate School of Science, Tohoku University, Sendai, 980-8578, Japan.

§Present address: Department of Chemistry, Simon Fraser University, Burnaby, British Columbia V5A 1S6, Canada.

their total summed energy were recorded for each event and added to the HPGe information off-line to provide fold k and sum-energy H information. High $k - H$ values, that retained ~60% (3.7×10^8 events) of the original data, were subsequently used in the off-line analysis to enhance the four-particle ^{135}Pr channel relative to competing five-particle (^{134}Pr, ^{134}Ce) and six-particle (^{133}Pr) channels. After this selection, the ratio of ^{135}Pr to ^{134}Pr was approximately doubled to 40% in the retained data.

Experimental Results. The thin-target data set was further unfolded into constituent triple (γ^3) coincidence events and replayed into a RADWARE-format [19] cube containing 1.8×10^9 events. In order to establish the multipolarity of the transitions, angular-intensity ratios were measured. The negative-parity yrast band of ^{135}Pr, obtained from this work, is shown in Fig. 1, while a double-gated γ-ray spectrum is presented in Fig. 2(a). The $I^\pi = 11/2^-$ state of ^{135}Pr is isomeric, with a half-life of 105 μs [20], and lies 317 keV above the $I^\pi = 3/2^+$ ground state [21]. The negative-parity yrast band of ^{135}Pr has been established firmly up to $I^\pi = 67/2^-$ and also extended to $I^\pi = (91/2^-)$. The work of Ref. [9] is confirmed up to $I^\pi = 47/2^-$, with eleven new transitions placed above this state. In addition, positive-parity sidebands [9] were confirmed up to $I^\pi = 39/2^+$ and $41/2^+$, but could not be significantly extended.

The yrast band of ^{134}Ce has also been extended by two transitions, to a tentative spin and parity $I^\pi = (38^+)$, from the present data; the level scheme is included in Fig. 1 and a double-gated spectrum is included in Fig. 2(b), where it can be seen that the topmost transitions have energies just above the previously known 1323 keV ($34^+ \to 32^+$) transition [12,13]. In addition, a weakly populated "superdeformed" band [22] has been confirmed in ^{134}Ce.

Discussion. Experimental data for negative-parity yrast bands in odd-Pr isotopes are presented in Fig. 3 in terms of total aligned angular momentum I_x and alignment i_x [23], plotted as a function of rotational frequency, $\omega \approx E_\gamma/2\hbar$. The yrast band of ^{134}Ce is also included in Fig. 3(a). In Fig. 3(b), a rotational reference, based on a configuration with a variable moment of inertia, $\mathcal{J}_{\rm ref} = \mathcal{J}_0 + \omega^2 \mathcal{J}_1$, has been subtracted in each case, with Harris parameters [24] $\mathcal{J}_0 = 17.0\hbar^2$ MeV^{-1} and $\mathcal{J}_1 = 25.8\hbar^4$ MeV^{-3} obtained from the S band of ^{130}Ce [25]. The data include ^{125}Pr [26], ^{127}Pr [27], ^{129}Pr [28], ^{131}Pr [29], ^{133}Pr [30], and ^{137}Pr [31], in addition to the new results for ^{135}Pr.

The yrast band of ^{135}Pr contains an odd-$h_{11/2}$ proton and hence the lowest-frequency alignment of $h_{11/2}$ quasiprotons is blocked. The large increase in i_x of 15$\hbar$ around $\omega = 0.45$ MeV/$\hbar$ in ^{135}Pr, as shown in Fig. 3(b), then suggests the rotational alignment of both the second and third $h_{11/2}$ quasiprotons and the first pair of $h_{11/2}$ quasineutrons. The simultaneous alignment of $\pi h_{11/2}$ and $\nu h_{11/2}$ quasiparticles has also been observed in ^{139}Pm [32]. In ^{134}Ce, the first pair of $h_{11/2}$ quasiprotons (blocked in ^{135}Pr) align at the lower frequency of $\omega \sim 0.35$ MeV/$\hbar$, with a sharp backbend, while the first pair of $h_{11/2}$ quasineutrons align at $\omega \sim 0.48$ MeV/$\hbar$; see Fig. 3(a). An increase in i_x around $\omega = 0.65$ MeV/$\hbar$ suggests further structural changes in both ^{135}Pr and ^{134}Ce.

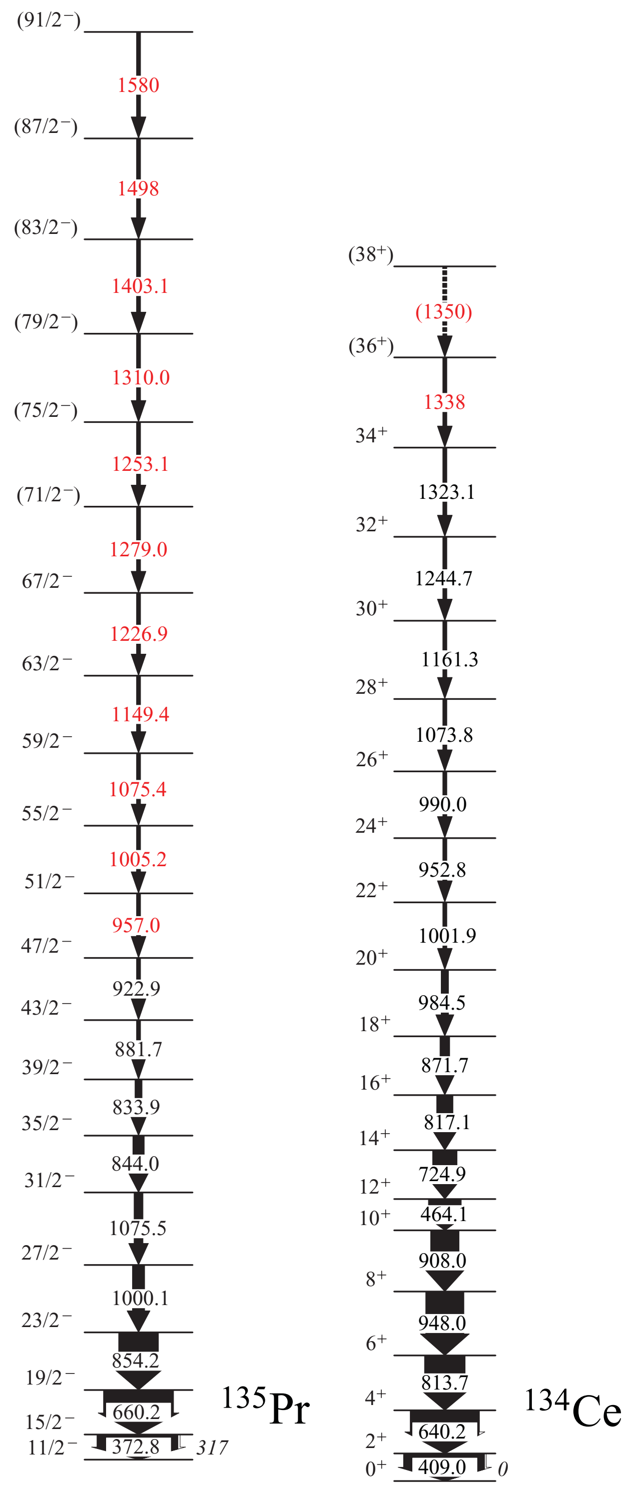

FIG. 1. (Color online) Partial level schemes deduced for ^{135}Pr and ^{134}Ce from the present experiment. Transition energies are given in keV and are accurate to ± 0.3 keV, except those quoted as integers, which are accurate to ± 1 keV. The transitions above $I^\pi = 47/2^-$ in ^{135}Pr and 34^+ in ^{134}Ce, labeled in red, are new.

Theoretical calculations for ^{135}Pr have been performed in the framework of the configuration-dependent cranked Nilsson-Strutinsky (CNS) formalism without pairing [33,34]. Results have been previously discussed for the mass 130 region

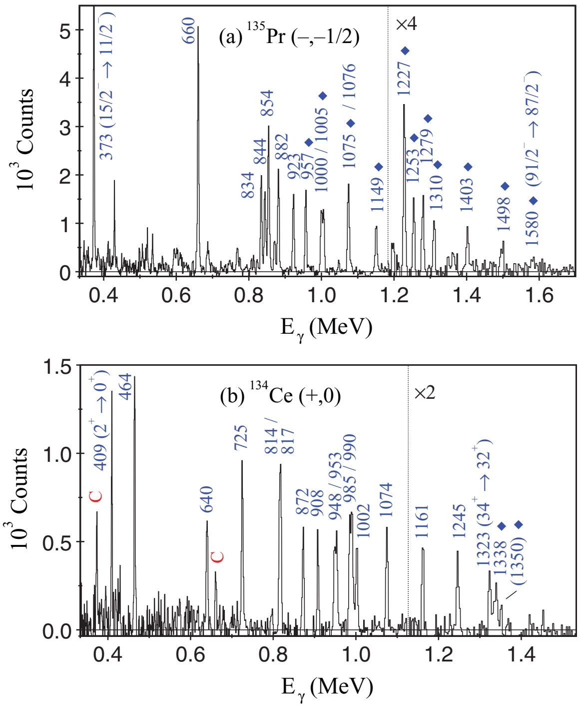

FIG. 2. (Color online) Coincident γ-ray spectra for (a) the $(\pi, \alpha) = (-, -1/2)$ yrast band in ^{135}Pr, and (b) the $(+, 0)$ yrast band in ^{134}Ce. Band members are labeled by their energies in keV, with new transitions denoted by diamonds. Contaminants from ^{135}Pr are labeled by "C" in (b).

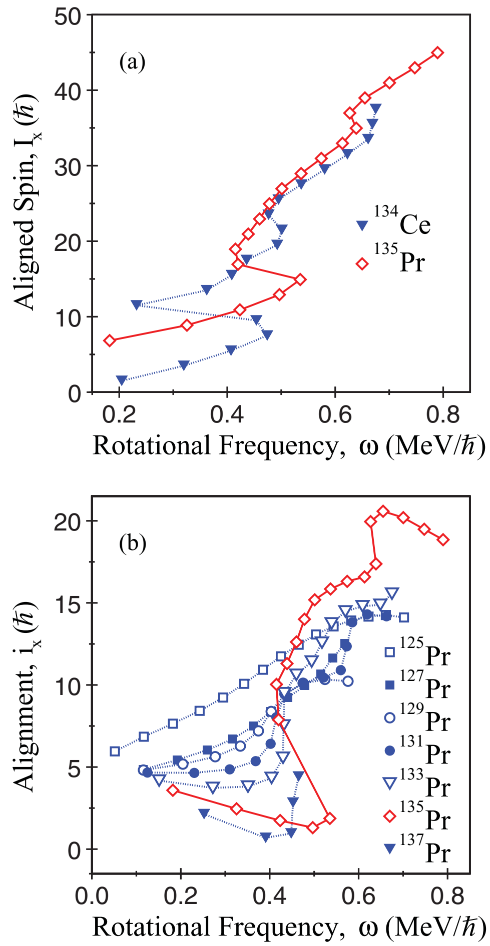

FIG. 3. (Color online) (a) Total aligned angular momentum I_x as a function of rotational frequency ω for the yrast bands in ^{135}Pr and ^{134}Ce. (b) Experimental alignment i_x as a function of rotational frequency ω for the negative-parity yrast bands in odd-A Pr isotopes.

in Ref. [35]. In the present calculations, we have used the updated formalism presented in Ref. [36] with $A = 150$ κ and μ parameters [37] defining the $\mathbf{l}\cdot\mathbf{s}$ and $\mathbf{l}^2$ strengths of the modified oscillator potential. Theoretical configurations are labeled, in relation to the ^{132}Sn core, using the shorthand notation $[p_1, n_1(n_2 n_3)]$. Here p_1 represents the number of $\pi h_{11/2}$ particles, relative to $Z = 50$, and n_1 represents the number of $\nu h_{11/2}$ holes, relative to $N = 82$. The numbers in parentheses are only labeled if nonzero, with n_2 and n_3 being, respectively, the number of neutrons in the $\nu h_{9/2}/f_{7/2}$ and $\nu i_{13/2}$ intruder orbitals from above the spherical $N = 82$ gap. The generalized configurations for structures in ^{135}Pr may be written in full as

$$\pi(d_{5/2}/g_{7/2})^{9-p_1}(h_{11/2})^{p_1}$$
$$\otimes\nu(d_{3/2}/s_{1/2})^{-(6+n_2+n_3-n_1)}(h_{11/2})^{-n_1}$$
$$\otimes\nu(h_{9/2}/f_{7/2})^{n_2}(i_{13/2})^{n_3}.$$

Note also that with many neutron holes in the $N_{\rm osc} = 4$ orbitals, some of them might be placed in orbitals of $d_{5/2}/g_{7/2}$ character.

Potential-energy surfaces for configurations with parity and signature $(\pi, \alpha) = (-, -1/2)$, fixed according to the observed high-spin band in ^{135}Pr, are presented for spin values $I = 75/2$ and $I = 91/2$ in Fig. 4. At the lower-spin value [see Fig. 4(a)], the energy minimum is found at a small deformation, $\varepsilon_2 \approx 0.12$, $\gamma \approx -35^\circ$, corresponding to the valence-space configuration [3,4] with a maximum spin value, $I_{\rm max} = 43.5$. Doppler-broadened line-shape analysis for the 1149-keV $(63/2^- \to 59/2^-)$ and 1227-keV $(67/2^- \to 63/2^-)$ transitions in ^{135}Pr (see Fig. 1) yields $Q_t \approx 3.3$ eb [11], compatible with this predicted triaxial shape. Around 0.5-MeV higher in energy, however, is a secondary minimum at $\varepsilon_2 \approx 0.27$, $\gamma \approx 15^\circ$, where configurations of the type [3,4(21)] and [3,4(22)] are calculated low in energy.

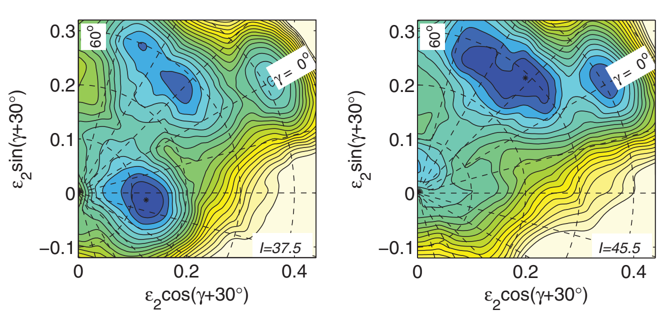

FIG. 4. (Color online) Calculated potential-energy surfaces for negative-parity configurations at spin values $I = 75/2$ and $91/2$ (signature, $\alpha = -1/2$). The contour line separation is 0.25 MeV.

At $I = 91/2$ [see Fig. 4(b)], corresponding to the highest spin value in the observed band, the larger-deformation minimum is calculated lowest in energy. Even though there is a close-to-spherical minimum, which comes only approximately 0.5-MeV higher in energy, it appears impossible that configurations corresponding to this shape could be assigned to the observed band, considering, for example, the I_{max} value of the [3,4] configuration. Indeed, the high-spin range of the observed band is well described by the core-excited configurations specified above with three or four neutrons excited across the $N = 82$ gap. Similar configurations with one $i_{13/2}$ neutron have been assigned to triaxial bands in nearby $_{60}$Nd isotopes; see Refs. [38,39]. An axial prolate minimum, with $\varepsilon_2 \approx 0.4$, $\gamma \approx 0^\circ$, also becomes competitive at the highest spins; see Fig. 4(b). This corresponds to the superdeformed shape (3:2 axes ratio) seen in ^{132}Ce and, indeed, ^{134}Ce [22].

In summary, the yrast band of ^{135}Pr has been significantly extended to over $40\hbar$, and that of ^{134}Ce to $38\hbar$. Cranking calculations suggest that these nuclei are γ soft and that configurations involving high-j orbitals intruding from above $N = 82$ are favored at the highest spins.

This work was supported in part by the UK Engineering and Physical Sciences Research Council, the US National Science Foundation, the US Department of Energy, and the Swedish Science Research Council.

[1] G. Andersson *et al.*, Nucl. Phys. A **268**, 205 (1976).
[2] I. Ragnarsson, A. Sobiczewski, R. K. Sheline, S. E. Larsson, and B. Nerlo-Pomorska, Nucl. Phys. A **233**, 329 (1974).
[3] Y. S. Chen, S. Frauendorf, and G. A. Leander, Phys. Rev. C **28**, 2437 (1983).
[4] E. S. Paul *et al.*, J. Phys. G **17**, 605 (1991).
[5] S. Frauendorf and F. R. May, Phys. Lett. B **125**, 245 (1983).
[6] G. A. Leander, S. Frauendorf, and F. R. May, in *Proceedings of the Conference on High Angular Momentum Properties of Nuclei, Oak Ridge, 1982*, edited by N. R. Johnson (Harwood, New York, 1983), p. 281.
[7] E. S. Paul, C. W. Beausang, D. B. Fossan, R. Ma, W. F. Piel Jr., N. Xu, L. Hildingsson, and G. A. Leander, Phys. Rev. Lett. **58**, 984 (1987).
[8] S. W. Ødegård *et al.*, Phys. Rev. Lett. **86**, 5866 (2001).
[9] T. M. Semkow *et al.*, Phys. Rev. C **34**, 523 (1986).
[10] S. Botelho *et al.*, Phys. Rev. C **58**, 3726 (1998).
[11] C. Fox, Ph.D. thesis, University of Liverpool, 2002.
[12] J. Gascon *et al.*, Niels Bohr Institute and Nordita 1989 Annual Report, 1990 (unpublished), p. 88.
[13] A. A. Sonzogni, Nucl. Data Sheets **103**, 1 (2004).
[14] J. Timár *et al.* (unpublished).
[15] P. J. Nolan and J. F. Sharpey-Schafer, Rep. Prog. Phys. **42**, 1 (1979).
[16] I. Y. Lee, Nucl. Phys. A **520**, 641c (1990).
[17] R. V. F. Janssens and F. S. Stephens, Nucl. Phys. News **6**, 9 (1996).
[18] M. Devlin, L. G. Sobotka, D. G. Sarantites, and D. R. LaFosse, Nucl. Instrum. Methods Phys. Res. A **383**, 506 (1996).
[19] D. C. Radford, Nucl. Instrum. Methods Phys. Res. A **361**, 297 (1995); **361**, 306 (1995).
[20] T. W. Conlon, Nucl. Phys. A **213**, 445 (1973).
[21] B. Singh, A. A. Rodionov, and Y. L. Khazov, Nucl. Data Sheets **109**, 517 (2008).
[22] N. J. O'Brien *et al.*, Phys. Rev. C **59**, 1334 (1999).
[23] R. Bengtsson and S. Frauendorf, Nucl. Phys. A **327**, 139 (1979).
[24] S. M. Harris, Phys. Rev. **138**, B509 (1965).
[25] D. M. Todd, R. Aryaeinejad, D. J. G. Love, A. H. Nelson, P. J. Nolan, P. J. Smith, and P. J. Twin, J. Phys. G **10**, 1407 (1984).
[26] A. N. Wilson *et al.*, Phys. Rev. C **66**, 021305 (2002).
[27] S. M. Mullins *et al.*, Phys. Rev. C **58**, R2626 (1998).
[28] B. H. Smith *et al.*, Phys. Lett. B **443**, 89 (1998).
[29] A. Galindo-Uribarri *et al.*, Phys. Rev. C **50**, R2655 (1994).
[30] E. S. Paul *et al.*, Nucl. Phys. A **690**, 341 (2001).
[31] N. Xu, C. W. Beausang, R. Ma, E. S. Paul, W. F. Piel Jr., D. B. Fossan, and L. Hildingsson, Phys. Rev. C **39**, 1799 (1989).
[32] N. Xu, C. W. Beausang, E. S. Paul, W. F. Piel Jr., P. K. Weng, D. B. Fossan, E. Gülmez, and J. A. Cizewski, Phys. Rev. C **36**, 1649 (1987).
[33] T. Bengtsson and I. Ragnarsson, Nucl. Phys. A **436**, 14 (1985).
[34] A. V. Afanasjev, D. B. Fossan, G. J. Lane, and I. Ragnarsson, Phys. Rep. **322**, 1 (1999).
[35] A. V. Afanasjev and I. Ragnarsson, Nucl. Phys. A **608**, 176 (1996).
[36] B. G. Carlsson and I. Ragnarsson, Phys. Rev. C **74**, 011302(R) (2006).
[37] T. Bengtsson, Nucl. Phys. A **512**, 124 (1990).
[38] S. Perriès *et al.*, Nucl. Phys. A **654**, 714c (1999).
[39] I. Ragnarsson, F. G. Kondev, E. S. Paul, M. A. Riley, and J. Simpson, Int. J. Mod. Phys. E **13**, 87 (2004).